Published in final edited form as:
Phys Med Biol. 2012 April 21; 57(8): 2273–2286. doi:10.1088/0031-9155/57/8/2273.

Characterizing the compression-dependent viscoelastic properties of human hepatic pathologies using dynamic compression testing

Ryan J. DeWall[1,2], **Shyam Bharat**[1], **Tomy Varghese**[1,2], **Meghan E. Hanson**[3], **Rashmi M. Agni**[4], and **Mark A. Kliewer**[3]

[1]Department of Medical Physics, University of Wisconsin-Madison

[2]Department of Biomedical Engineering, University of Wisconsin-Madison

[3]Department of Radiology, University of Wisconsin-Madison

[4]Department of Pathology and Laboratory Medicine, University of Wisconsin-Madison

Abstract

Recent advances in elastography have provided several imaging modalities capable of quantifying the elasticity of tissue, an intrinsic tissue property. This information is useful for determining tumour margins but may also provide information to diagnose specific tumour types. In this study, we used dynamic compression testing to quantify the viscoelastic properties of 16 human hepatic primary and secondary malignancies and their corresponding background tissue obtained following surgical resection. Two additional backgrounds were also tested. An analysis of the background tissue showed that F4-graded fibrotic liver tissue was significantly stiffer than F0-graded tissue, with a modulus contrast of 4:1. Steatotic liver tissue was slightly stiffer than normal liver tissue, but not significantly so. The tumour-to-background storage modulus contrast of hepatocellular carcinomas, a primary tumour, was approximately 1:1, and the contrast decreased with increasing fibrosis grade of the background tissue. Ramp testing showed that the background stiffness increased faster than the malignant tissue. Conversely, secondary tumours were typically much stiffer than the surrounding background, with a tumour-to-background contrast of 10:1 for colon metastases and 10:1 for cholangiocarcinomas. Ramp testing showed that colon metastases stiffened faster than their corresponding background. These data have provided insights into the mechanical properties of specific tumour types, which may prove beneficial as the use of quantitative stiffness imaging increases.

Keywords

dynamic compression testing; elastography; hepatic malignancies; storage modulus; ultrasound

1. Introduction

Pathological changes to tissue are often accompanied by structural changes that lead to an increase in tissue stiffness (Fung, 1993). For example, breast or prostate tumours often exhibit increased stiffness with respect to the surrounding tissue. Physicians often exploit this stiffness differential to locate tumours using manual palpation. This phenomenon is also observed in the liver. Inflammation caused by liver disease results in a progressive

Address all correspondence to: Ryan DeWall, Department of Medical Physics, 1122 S1 WIMR, 1111 Highland Ave, Madison, WI 53705, Voice: (616) 405-9172, Fax: (608) 262-2413, dewall@wisc.edu, tvarghese@wisc.edu.

replacement of normal tissue with fibrous scar tissue (Bruix *et al.*, 2001), leading to an increase in tissue stiffness (Salameh *et al.*, 2009). Hepatic malignancies may also be stiff with respect to the surrounding tissue. However, these tumours are difficult to detect with manual palpation alone because of overlying fat and tissue layers.

Elastography is a form of virtual palpation used to differentiate tissue with differing stiffness and has been used to image lesions that cannot be detected with manual palpation alone, such as stiffer masses in the liver. For example, sonoelastography has delineated stiff thermal ablations *ex vivo* (Zhang *et al.*, 2008). Strain imaging has been used to demarcate radiofrequency ablations *ex vivo* and *in vivo*, using the ablation electrode as the compression device (Bharat *et al.*, 2008; Rubert *et al.*, 2010; Liu *et al.*, 2006). Recently, acoustic radiation force imaging (ARFI) has been used to determine hepatic malignancy margins by "pushing" the tissue with an acoustic pulse and measuring the resulting displacements. The stiffer malignant tissue displaces less than the softer background (Fahey *et al.*, 2008a; Fahey *et al.*, 2008b).

Boundary delineation of hepatic malignancies is important, but assessing the pathological state of tumour and background tissue is just as critical. Strain and displacement imaging provide margin information but do not provide information on the intrinsic stiffness of the tumour and surrounding background. Tissue elasticity (i.e. the Young's Modulus) provides quantitative information, and several new imaging modalities have been developed to estimate this parameter. Magnetic resonance elastography (MRE) has successfully been used to quantify the Young's Modulus in a variety of cancer types (Venkatesh *et al.*, 2008), as well as stage fibrosis (Huwart *et al.*, 2006; Asbach *et al.*, 2008). ARFI shear wave tracking has obtained quantitative estimates of the shear wave velocity, which is proportional to the Young's Modulus, within regions of interest in hepatic malignancies and in healthy tissue (Kapoor *et al.*, 2011; Palmeri *et al.*, 2008). Supersonic shear imaging (SSI) and two dimensional transient elastography have successfully been used to quantify the Young's Modulus in breast malignancies (Bercoff *et al.*, 2003; Tanter *et al.*, 2008) and in healthy liver tissue (Muller *et al.*, 2009), and electrode vibration elastography has quantified shear wave velocity within radiofrequency ablations (DeWall *et al.*, 2011b). These techniques are exciting advances in elastography and could aid in diagnosing hepatic malignancies.

Imaging studies have shown promise in quantifying the elasticity in hepatic malignancies, but mechanical testing will help corroborate results. Many studies have investigated the mechanical properties of normal liver tissue in animal models. The strain-rate dependent behaviour of bovine liver tissue has been investigated (Pervin *et al.*, 2011; Roan and Vemaganti, 2011). In a porcine model, the effects of perfusion on liver tissue mechanics has been studied (Kerdok *et al.*, 2006), and one dimensional transient elastography stiffness estimates have been compared to dynamic mechanical analysis (Chatelin *et al.*, 2011). Dynamic compression testing has also been used to quantify the viscoelastic properties of normal and ablated canine hepatic tissue (Kiss *et al.*, 2004; Kiss *et al.*, 2009).

However, few studies have estimated the mechanical properties of human liver tissue via mechanical testing. An aspiration device has been developed to quantify liver stiffness on the liver surface during open surgery (Mazza *et al.*, 2007). Other studies have quantified the stiffness of the human liver based on fibrosis score (Kusaka *et al.*, 2000; Yeh *et al.*, 2002), as well as the stiffness of cancers, namely a cholangiocarcinoma and a focal nodular hyperplasia (Yeh *et al.*, 2002). However, only these two human hepatic lesions were tested, and only simple cyclic testing was performed. The viscoelastic properties of hepatic malignancies have been poorly studied via mechanical testing, and few different types of cancers have been investigated.

To gain insights into possible correlations between the mechanical properties of human hepatic malignancies and cancer type, more work is necessary. In this study, we quantify the mechanical properties of human primary and secondary malignancies and their corresponding background tissue using dynamic compression testing through a range of precompressional loads and testing frequencies. In addition, we investigate the effects of strain hardening on hepatic malignancies and background tissue through a broad compression range using ramp testing. Background tissue samples are compared based on fibrosis grade or steatosis to determine differences in the viscoelastic properties based on the pathological state of the tissue.

2. Methods

2.1 Experiment

Malignant and background hepatic tissue samples from 18 patients were obtained from the University of Wisconsin Pathology Laboratory. Each sample came from a patient who underwent a surgical resection, and all surgeries were performed at the University of Wisconsin Hospital and Clinics (Madison, WI). Following surgery, the liver section was brought to the Surgical Pathology Laboratory. Approximately 1 cm^3 of the lesion and 1 cm^3 of the background were removed, placed in saline, and transported to our laboratory for dynamic compression testing. For two of the cases, only background tissue was obtained and tested (i.e. 16 lesions were tested and 18 backgrounds). Pathology types are listed in Table 1. Samples were typically tested within two hours of acquisition and were refrigerated until testing. Before testing, samples were raised to room temperature. If necessary, samples were further shaped to make them square. The dimensions of all sides were measured multiple times and averaged. All protocols and procedures for this study were approved by the University of Wisconsin Institutional Review Board for studies on excised tissue specimens.

2.2 Dynamic Compression Testing

To quantify the viscoelastic properties of the benign, malignant, and background tissue, dynamic compression tests were performed. This testing has been previously described (Kiss *et al.*, 2006; DeWall *et al.*, 2010). Briefly, an acrylic platen induces a sinusoidal displacement, or strain, on the tissue sample, resulting in a sinusoidal force, or stress, phase-shifted by an angle δ. The complex modulus (E*) is the ratio of the stress to the strain, which can be divided into the energy stored per cycle, or storage modulus (E'), and the energy lost per cycle, or loss modulus (E''). The ratio of these two quantities is often referred to as tan δ, or viscous damping (Lakes, 1999):

$$\tan\delta = \frac{E''}{E'}. \quad (1)$$

All samples were dynamically tested using an EnduraTEC ELF 3220 (Bose Corporation, EnduraTEC Systems Group; Minnetonka, MN). The samples and testing platens were coated with a thin layer of mineral oil to minimize tissue desiccation and friction at the contact surfaces. The upper platen was lowered until just touching the upper surface of the tissue sample. After contact was established, the sample was dynamically tested with sinusoidal compressions over a range of compressions and frequencies.

The system was controlled using the ELF dynamic mechanical analysis (DMA) software. Each sample was tested from 1% to 6% precompression with a compression amplitude of 2%. For example, a sample tested at 1% precompression was sinusoidally tested from 1% to 3% compression with a mean compression of 2%. For each precompression level, samples were dynamically tested at 1, 10, 20, and 30 Hz. In order to precondition the tissue (Fung,

1993), several compression cycles occurred before data collection. There was a 15 second hold between testing frequencies. During this time, the sample was held at the mean strain value (e.g. 2% for 1–3% compression test). For each testing frequency, the DMA software measured the force amplitude, displacement amplitude, and phase lag at the peak frequency and output |E*|, E′, E″, and tan δ. The DMA software assumes that the area of the sample faces remains the same. Because tissue is nearly incompressible, a correction factor was applied to account for the changes in sample face size with compression.

During the course of this study, it was observed that the tumour-to-background contrast changed little in the 1–6% precompression range. Simple ramp testing was added to the protocol to investigate strain hardening at higher levels of compression. After dynamic testing, samples were compressed up to 20% precompression at a strain rate of 0.1 %/s. Three cycles of data were collected to precondition the tissue, as the third cycle onward has been shown to be repeatable (Fung, 1993). The sample face area changes because the tissue is nearly incompressible. This must be accounted for in the calculation of stress and strain. Material stretch is defined as:

$$\lambda = \frac{h}{h_0}. \tag{2}$$

The Cauchy stress is

$$\sigma = \frac{F}{A_0}\lambda \tag{3}$$

and the Almansi strain is

$$\varepsilon = \frac{1}{2}\left(1 - \frac{1}{\lambda^2}\right). \tag{4}$$

2.3 Statistics

The significance of the overall changes in E′, E″ and tan δ over the precompression range and the frequency range was assessed using a one-way analysis of variance (ANOVA; $p < 0.001$). Tukey multiple comparisons were used to compare E′, E″, and tan δ at each precompression level or frequency to E′, E″, and tan δ at 1% precompression or 1 Hz frequency, respectively (*, $p < 0.05$; **, $p < 0.001$). Significance between groups (e.g. malignant vs. background tissue) at each precompression level or frequency was also tested (†, $p < 0.05$; ‡, $p < 0.001$). All results are presented as mean ± standard deviation.

3. Results

Background tissue stiffness was compared by grouping samples based on fibrosis grade or steatosis. Figure 1 shows background tissue broken down into F0 (n = 14), F2 (n = 2), and F4 (n = 2) fibrosis grades. The F4-graded liver tissue storage modulus was significantly higher than that of F0 tissue, with a ratio of approximately 4:1. In Figure 2, samples were grouped as steatotic or normal, excluding the cirrhotic (F4-graded) samples. Steatotic tissue exhibited an elevated storage modulus with respect to normal tissue, but was not significantly so, except for the 3% compression level. The loss modulus was also elevated but not significantly so.

The effect of precompression on hepatic tissue viscoelastic properties was investigated in benign and malignant lesions and the surrounding background tissue. Figure 3 shows dynamic compression testing data from hepatocellular carcinomas (HCCs, n = 4), a primary cancer. There was a trend of increasing stiffness with increasing precompression in figure 3(a). The storage modulus of the background was more variable than that of the HCCs tested. The tumour-to-background contrast was broken down by fibrosis grade in figure 3(b) and decreased from 1.5:1 at F0 to 0.5:1 at F4. Tan δ changed little with increasing precompression. In figure 4, the storage modulus of colon metastases (n = 6), a secondary cancer, was significantly higher than the background tissue and was more variable. The tumour-to-background contrast was relatively constant at 10:1 for F0 background and was approximately 1.25:1 for the one F2 background that was tested. As with HCCs, tan δ changed little with precompression. In figure 5, the storage modulus of cholangiocarcinomas (n = 3), another secondary cancer, was highly variable, but not so in the background tissue. The tumour-to-background contrast was approximately 10:1, and tan δ was relatively constant. A benign adenoma (n = 1), gastrointestinal stromal metastasis (n = 1), and neuroendocrine metastasis (n = 1) are presented in figure 6. All exhibited increases in stiffness with increasing precompression, and the tumour-to-background contrast ranged from 1.5 to 2.5 for all lesions.

Malignant and background liver tissue also exhibited frequency-dependent behaviour. Figure 7 presents the storage modulus and tan δ in HCCs and their corresponding background for the 1–3% and 6–8% compression levels. The storage modulus in HCCs and background tissue increased with precompression, although not significantly. Tan δ increased significantly with increasing frequency in both background and malignant tissue. The storage modulus contrast and tan δ contrast remained relatively constant across frequencies. In figure 8, the stiffness of colon metastases was significantly higher than the background tissue for all frequencies at the 1–3% and 6–8% compression levels. The storage modulus tended to increase with increasing frequency, although not significantly so. Tan δ significantly increased with increasing frequency in the background tissue. As with HCCs, the tumour-to-background contrast was relatively constant.

Ramp loading up to 20% compression was used to investigate strain hardening in HCCs and colon metastases when compared to the surrounding background. The background of all samples that were tested had a fibrosis grade of F0. Interestingly, the background strain-hardened faster than the HCC that was tested, as shown in figure 9. In figure 10, all colon metastases (n = 4) strain-hardened faster than the surrounding background, but the rate and extent of strain-hardening was quite variable.

4. Discussion

We have quantified differences in tissue stiffness contrast based on cancer type or the background tissue disease state. Few studies have quantified tissue mechanics in human hepatic malignancies via mechanical testing (Yeh *et al.*, 2002; Kusaka *et al.*, 2000). This work provides mechanical testing estimates of the viscoelastic properties of specific cancer types that are currently absent from the literature. HCCs, a primary tumour, were approximately the same contrast as the surrounding background and interestingly, exhibited lower contrast with large compressions. Metastases, or secondary cancers, were stiffer than the surrounding background. Tumours also strain-hardened faster than their corresponding background liver tissue. Cirrhotic F4-graded tissue was significantly stiffer than F0-graded tissue, and mean values of the graded sample groups were comparable to estimates obtained via elastography (Sandrin *et al.*, 2003). Steatotic tissue was only slightly stiffer than normal tissue but generally not significantly so, as shown in a prior study on liver tissue in rats

(Salameh *et al.*, 2009). These results provide insights that may prove useful in diagnosing hepatic malignancies using quantitative stiffness imaging modalities.

The background tissue samples were divided into groups based on fibrosis score or the presence or absence of steatosis. F4-graded cirrhotic tissue was significantly stiffer than normal background tissue, and results were comparable to those previously reported (Sandrin *et al.*, 2003; Palmeri *et al.*, 2008). The variability of tissue stiffness increased with fibrosis grade, likely the result of increases in tissue heterogeneity with pathological state. Elastography modalities such as SSI and MRE can partially circumvent increases in dispersion resulting from heterogeneity by averaging the stiffness in a large ROI. This was not possible with our system, because the testing platens could not accommodate a sample larger than 1 cm^3. However, the mean elastic moduli were comparable to imaging studies. Steatotic tissue was stiffer than normal tissue, but not significantly so, as reported in prior studies (Yeh *et al.*, 2002). ARFI shear wave imaging has also shown stiffness increases with steatosis in a chicken model (Guzman Aroca *et al.*, 2010). The loss modulus was also elevated, but not significantly. This differs from observations in a rat model of steatosis (Salameh *et al.*, 2009). However, in that study, the level of steatosis was approximately 30%, while the level of steatosis observed in this study was only 5% to 10%.

We tested four HCCs, primary cancers, over the course of this study. The storage modulus in the tumours was approximately the same stiffness as the corresponding background. One study reported that testing an HCC was impossible because it was too soft (Yeh *et al.*, 2002); we did not find this to be the case, but the HCCs were relatively soft compared to the background when compared to other tissue types. This may be explained by the fact that HCCs primarily occur in patients with liver fibrosis, which results from a variety of diseases or conditions including hepatitis B and C, diabetes mellitus, alcoholism, and fat accumulation (Bruix *et al.*, 2001). Damage to the liver leads to a progressive replacement of normal tissue with scar tissue, increasing the inherent stiffness of the liver. Of our samples, two were graded F0, one was graded F2, and one was graded F4, which is reflected in the variability of the background tissue. In figure 3b, the contrast is broken down based on fibrosis grade. Tumour-to-background contrast is relatively low and decreases with increasing fibrosis grade, with the tumour being softer than the surrounding background (0.5:1) for F4-graded tissue. Low contrast or tumours softer than the surrounding background may be a useful indicator of primary hepatic cancer. Interestingly, tan δ values and variability were similar for both malignant and background tissue, similar to those previously reported in healthy animal tissue (Chatelin *et al.*, 2011; Kiss *et al.*, 2004).

Secondary tumours were in general stiffer than their corresponding background. Colon metastases were significantly stiffer and much more variable than the background tissue. The same behaviour was observed for cholangiocarcinomas. The variability may reflect different levels of tumour progression, patient variability (e.g. health, diet), or tissue heterogeneity resulting from the pathological state of the tissue. Ideally, we would have globally tested the entire tumour or spatially mapped the tissue stiffness via dynamic indentation (Dewall *et al.*, 2011a). However, due to the finite amount of tissue available and the pathology lab's need to analyze tissue for pathological diagnosis, we could not acquire entire tumours. In addition, for our compression testing protocol, it is infeasible to test tumours at the same level of progression in human studies, as treatment strategies are started soon after tumour detection. Interestingly, the background tissue storage modulus estimates were very consistent across the secondary tumours tested, which reflects the fact that the tumour metastasized from another site. That is, the liver did not have an underlying disease or condition that caused the cancer: of the colon metastases (n = 6) and cholangiocarinomas (n = 3) tested, eight were graded F0 and one was graded F2. Tan δ estimates and variability were again comparable, indicating that viscous damping may not hold any diagnostic value.

We acquired only one of several types of the lesions that were tested, including a benign adenoma, gastrointestinal stromal tumour metastasis, and neuroendocrine metastasis. All three were comparably stiff, which may suggest some tumours are difficult to differentiate based on stiffness information. However, only one sample was obtained for each case, which makes generalized conclusions difficult. Acquiring more samples would have been ideal, but the probability of acquiring more of these less common cancer types was low; only one of each of these cancer types was acquired over the duration of this three and a half year study.

Both HCCs and colon metastases showed similar frequency-dependent behaviour. The storage modulus and tan δ increased with increasing frequency, following the expected trend. However, the stiffness of the tumour and background tissue at all frequencies remained relatively constant, having little effect on the observed contrast. This may not be true of higher testing frequencies, which is applicable to radiation-force based elastography approaches that operate in the range of 50–400 Hz (Muller *et al.*, 2009; Sandrin *et al.*, 2003). We did not estimate the viscoelastic tissue properties at higher frequencies through the course of this study. Future studies should investigate what, if any, effect higher frequencies have on the tumour-to-background contrast.

Tumour-to-background contrast for all tumour types changed little up to 6% precompression. Ramp testing elucidated the strain hardening behaviour of the tissue at higher levels of compression. Interestingly, contrast decreased in the HCC that was tested. That is, it became softer relative to the background, which is likely the result of the stiff fibrotic tissue in the background. Colon metastases all strain-hardened faster than the corresponding background but at different rates. Strain hardening may be useful to increase tumour-to-background contrast in secondary tumours, but achieving a high enough level of compression may be difficult in a clinical setting. Additionally, the compression will strain harden the overlying layers of tissue, which may obscure rather than clarify the image. Adding a specified amount of compression by hand is also difficult to control or quantify, decreasing the value of the quantitative stiffness estimates obtained.

There are inherent limitations to *ex vivo* experiments. Some have shown differences between *ex vivo* and *in vivo* measurements, which may result from tissue degradation over time (Chatelin *et al.*, 2011). However, in this study, we tested tissue samples soon after removal from the patient, which minimized this effect. *In vivo* tissue is also actively perfused, which has been shown to affect the observed tissue stiffness (Kerdok *et al.*, 2006), but perfusing the small tissue samples (~1 cm^3) that we obtained would have been impossible. These two factors should be considered, but both the lesion and background absolute stiffness may change at the same rate. That is, the tumour-to-background contrast may be the same regardless of whether the stiffness was measured *ex vivo* or *in vivo*, despite absolute differences in the tumour and background tissue. In future studies, it would be beneficial to use a quantitative stiffness imaging modality to quantify tumour and background stiffness before resection, followed by *ex vivo* dynamic testing after resection. However, during the course of this study, these systems were not available to us.

We have characterized the viscoelastic properties of human primary and secondary cancers via mechanical testing, which few previous studies have quantified. Tumour-to-background contrast was much lower in primary than in secondary cancers. This observation may prove beneficial if stiffness maps of hepatic malignancies can be visualized in a repeatable manner. With the advent of new imaging modalities that can quantify the elasticity in tumour and background tissue noninvasively, this may soon be a clinical reality.

Acknowledgments

Funding support was provided by NIH grants R01 CA112192-04, R01 CA112192-S103, and T32 CA09206-31.

References

Asbach P, Klatt D, Hamhaber U, Braun J, Somasundaram R, Hamm B, Sack I. Assessment of liver viscoelasticity using multifrequency MR elastography. Magn Reson Med. 2008; 60:373–9. [PubMed: 18666132]

Bercoff J, Chaffai S, Tanter M, Sandrin L, Catheline S, Fink M, Gennisson JL, Meunier M. In vivo breast tumor detection using transient elastography. Ultrasound Med Biol. 2003; 29:1387–96. [PubMed: 14597335]

Bharat S, Varghese T, Madsen EL, Zagzebski JA. Radio-frequency ablation electrode displacement elastography: a phantom study. Medical Physics. 2008; 35:2432–42. [PubMed: 18649476]

Bruix J, Sherman M, Llovet JM, Beaugrand M, Lencioni R, Burroughs AK, Christensen E, Pagliaro L, Colombo M, Rodes J. Clinical management of hepatocellular carcinoma. Conclusions of the Barcelona-2000. EASL conference. European Association for the Study of the Liver. J Hepatol. 2001:35421–30.

Chatelin S, Oudry J, Perichon N, Sandrin L, Allemann P, Soler L, Willinger R. In vivo liver tissue mechanical properties by transient elastography: Comparison with dynamic mechanical analysis. Biorheology. 2011; 48:75–88. [PubMed: 21811013]

Dewall R, Varghese T, Brace C. Quantifying Local Stiffness Variations in Radiofrequency Ablations with Dynamic Indentation. IEEE Trans Biomed Eng. 2011a

DeWall RJ, Varghese T, Kliewer MA, Harter JM, Hartenbach EM. Compression-dependent viscoelastic behavior of human cervix tissue. Ultrason Imaging. 2010; 32:214–28. [PubMed: 21213567]

DeWall RJ, Varghese T, Madsen EL. Shear wave velocity imaging using transient electrode perturbation: phantom and ex vivo validation. IEEE Trans Med Imaging. 2011b; 30:666–78. [PubMed: 21075719]

Fahey BJ, Nelson RC, Bradway DP, Hsu SJ, Dumont DM, Trahey GE. In vivo visualization of abdominal malignancies with acoustic radiation force elastography. Phys Med Biol. 2008a; 53:279–93. [PubMed: 18182703]

Fahey BJ, Nelson RC, Hsu SJ, Bradway DP, Dumont DM, Trahey GE. In vivo guidance and assessment of liver radio-frequency ablation with acoustic radiation force elastography. Ultrasound Med Biol. 2008b; 34:1590–603. [PubMed: 18471954]

Fung, YC. Biomechanics: Mechanical Properties of Living Tissues. New York: Springer; 1993. p. 242-320.

Guzman Aroca F, Ayala I, Serrano L, Berna-Serna JD, Castell MT, Garcia-Perez B, Reus M. Assessment of liver steatosis in chicken by using acoustic radiation force impulse imaging: preliminary results. Eur Radiol. 2010; 20:2367–71. [PubMed: 20445981]

Huwart L, Peeters F, Sinkus R, Annet L, Salameh N, ter Beek LC, Horsmans Y, Van Beers BE. Liver fibrosis: non-invasive assessment with MR elastography. NMR Biomed. 2006; 19:173–9. [PubMed: 16521091]

Kapoor A, Mahajan G, Sidhu BS, Lakhanpal VP. Real-time elastography in differentiating metastatic from nonmetastatic liver nodules. Ultrasound Med Biol. 2011; 37:207–13. [PubMed: 21257087]

Kerdok AE, Ottensmeyer MP, Howe RD. Effects of perfusion on the viscoelastic characteristics of liver. J Biomech. 2006; 39:2221–31. [PubMed: 16126215]

Kiss MZ, Daniels MJ, Varghese T. Investigation of temperature-dependent viscoelastic properties of thermal lesions in ex vivo animal liver tissue. J Biomech. 2009; 42:959–66. [PubMed: 19362313]

Kiss MZ, Hobson MA, Varghese T, Harter J, Kliewer MA, Hartenbach EM, Zagzebski JA. Frequency-dependent complex modulus of the uterus: preliminary results. Physics in Medicine and Biology. 2006; 51:3683–95. [PubMed: 16861774]

Kiss MZ, Varghese T, Hall TJ. Viscoelastic characterization of in vitro canine tissue. Phys Med Biol. 2004; 49:4207–18. [PubMed: 15509061]

Kusaka K, Harihara Y, Torzilli G, Kubota K, Takayama T, Makuuchi M, Mori M, Omata S. Objective evaluation of liver consistency to estimate hepatic fibrosis and functional reserve for hepatectomy. J Am Coll Surg. 2000; 191:47–53. [PubMed: 10898183]

Lakes, R. Viscoelastic Solids. Boca Raton: CRC Press; 1999. p. 1-72.

Liu W, Zagzebski JA, Varghese T, Dyer CR, Techavipoo U, Hall TJ. Segmentation of elastographic images using a coarse-to-fine active contour model. Ultrasound Med Biol. 2006; 32:397–408. [PubMed: 16530098]

Mazza E, Nava A, Hahnloser D, Jochum W, Bajka M. The mechanical response of human liver and its relation to histology: an in vivo study. Med Image Anal. 2007; 11:663–72. [PubMed: 17719834]

Muller M, Gennisson JL, Deffieux T, Tanter M, Fink M. Quantitative viscoelasticity mapping of human liver using supersonic shear imaging: preliminary in vivo feasibility study. Ultrasound Med Biol. 2009; 35:219–29. [PubMed: 19081665]

Palmeri ML, Wang MH, Dahl JJ, Frinkley KD, Nightingale KR. Quantifying hepatic shear modulus in vivo using acoustic radiation force. Ultrasound in Medicine & Biology. 2008; 34:546–58. [PubMed: 18222031]

Pervin F, Chen WW, Weerasooriya T. Dynamic compressive response of bovine liver tissues. J Mech Behav Biomed Mater. 2011; 4:76–84. [PubMed: 21094481]

Roan E, Vemaganti K. Strain rate-dependent viscohyperelastic constitutive modeling of bovine liver tissue. Med Biol Eng Comput. 2011; 49:497–506. [PubMed: 21052853]

Rubert N, Bharat S, DeWall RJ, Andreano A, Brace C, Jiang J, Sampson L, Varghese T. Electrode displacement strain imaging of thermally-ablated liver tissue in an in vivo animal model. Med Phys. 2010; 37:1075–82. [PubMed: 20384243]

Salameh N, Larrat B, Abarca-Quinones J, Pallu S, Dorvillius M, Leclercq I, Fink M, Sinkus R, Van Beers BE. Early detection of steatohepatitis in fatty rat liver by using MR elastography. Radiology. 2009; 253:90–7. [PubMed: 19587308]

Sandrin L, Fourquet B, Hasquenoph JM, Yon S, Fournier C, Mal F, Christidis C, Ziol M, Poulet B, Kazemi F, Beaugrand M, Palau R. Transient elastography: a new noninvasive method for assessment of hepatic fibrosis. Ultrasound in Medicine & Biology. 2003; 29:1705–13. [PubMed: 14698338]

Tanter M, Bercoff J, Athanasiou A, Deffieux T, Gennisson JL, Montaldo G, Muller M, Tardivon A, Fink M. Quantitative assessment of breast lesion viscoelasticity: initial clinical results using supersonic shear imaging. Ultrasound Med Biol. 2008; 34:1373–86. [PubMed: 18395961]

Venkatesh SK, Yin M, Glockner JF, Takahashi N, Araoz PA, Talwalkar JA, Ehman RL. MR elastography of liver tumors: preliminary results. AJR Am J Roentgenol. 2008; 190:1534–40. [PubMed: 18492904]

Yeh WC, Li PC, Jeng YM, Hsu HC, Kuo PL, Li ML, Yang PM, Lee PH. Elastic modulus measurements of human liver and correlation with pathology. Ultrasound Med Biol. 2002; 28:467–74. [PubMed: 12049960]

Zhang M, Castaneda B, Christensen J, Saad W, Bylund K, Hoyt K, Strang JG, Rubens DJ, Parker KJ. Real-time sonoelastography of hepatic thermal lesions in a swine model. Med Phys. 2008; 35:4132–41. [PubMed: 18841866]

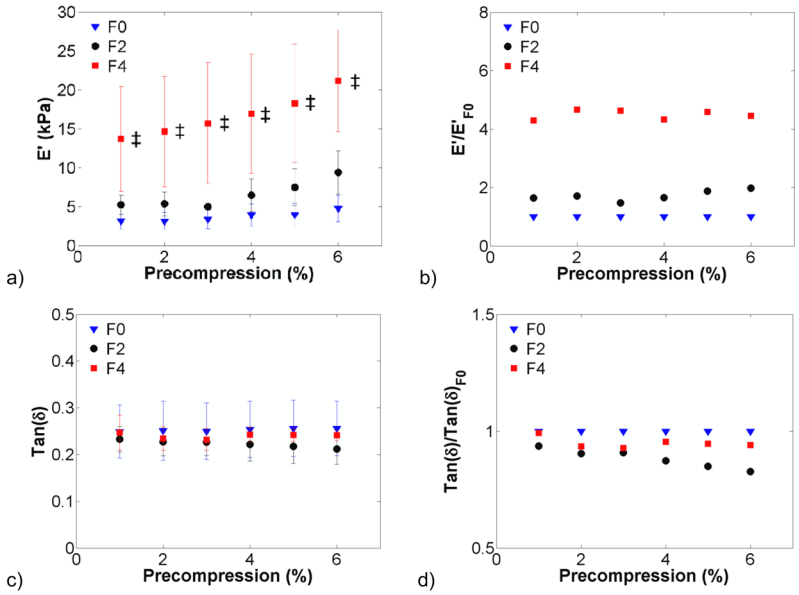

Figure 1.

Viscoelastic properties of background tissue based on fibrosis score. The storage modulus (a) increased with increasing fibrosis score. The storage modulus normalized to F0 grade (b) was roughly four times higher in F4 cases. Tan δ (c) remained relatively constant regardless of fibrosis grade. There was little difference among fibrosis grades when tan δ was normalized to F0 (d).

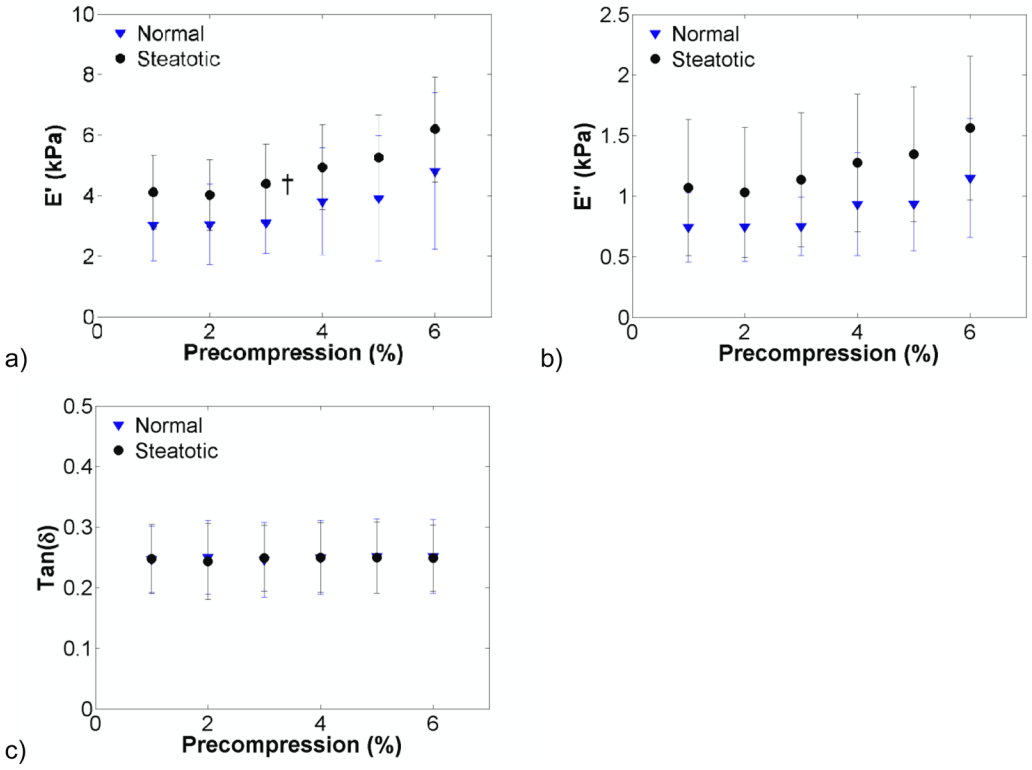

Figure 2.

Effects of precompression on normal (n = 10) and steatotic (n = 6) liver tissue. The storage modulus (a) of steatotic liver was not significantly higher than normal tissue for all compression levels but 3 percent (†, $p<0.05$; ‡, $p<0.001$), although the mean stiffness was slightly elevated with respect to normal. The loss modulus (b) in steatotic tissue was elevated with respect to normal tissue but not significantly so. The tan δ of steatotic or normal tissue (c) was relatively constant with increasing precompression.

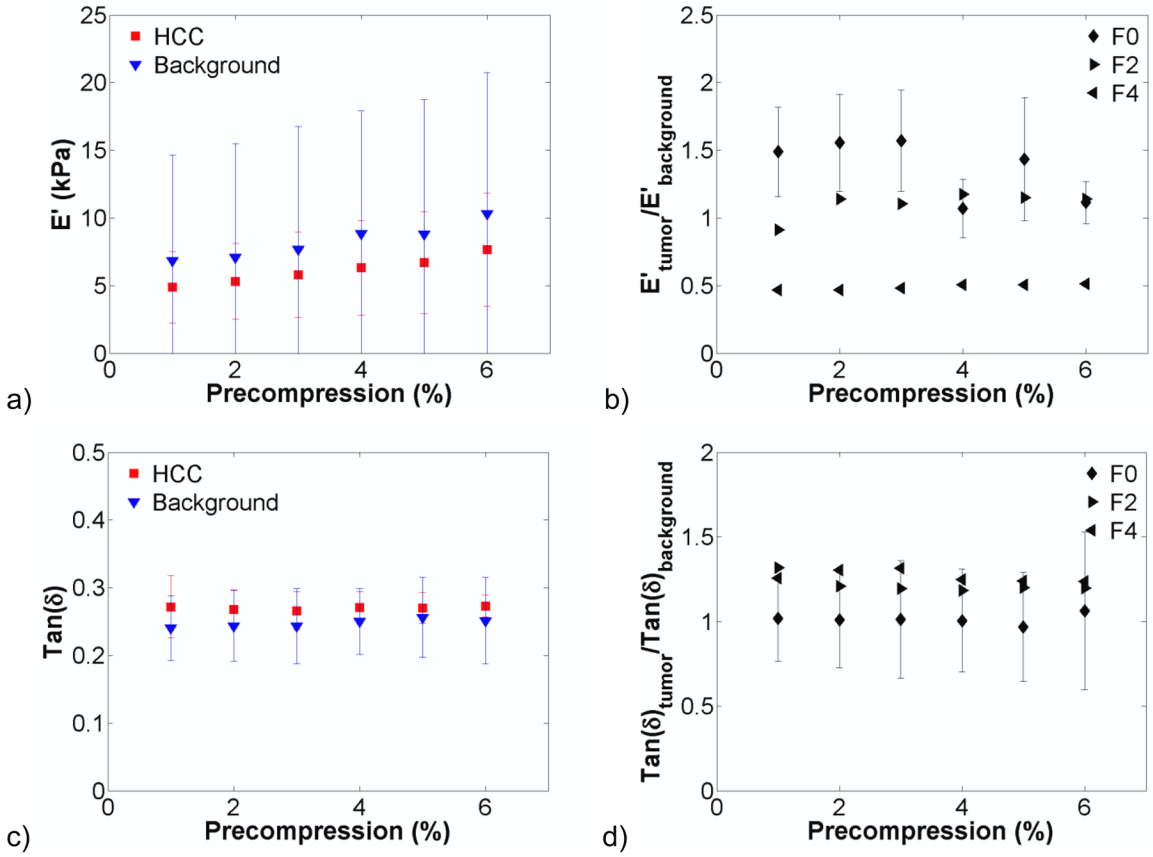

Figure 3.

Viscoelastic properties of hepatocellular carcinomas (HCCs) and surrounding background tissue (n = 4). Storage modulus (a) for HCCs and background tissue increased with increasing precompression. The background tissue was highly variable because of different fibrosis grades. Underlying tissue contrast (b) remained relatively constant with compression, but decreased with increasing fibrosis grade (F0, n = 2; F2, n = 1; F4, n = 1). Tan(δ) (c) and tan(δ) tumour-to-background contrast (d) remained relatively constant with increasing compression.

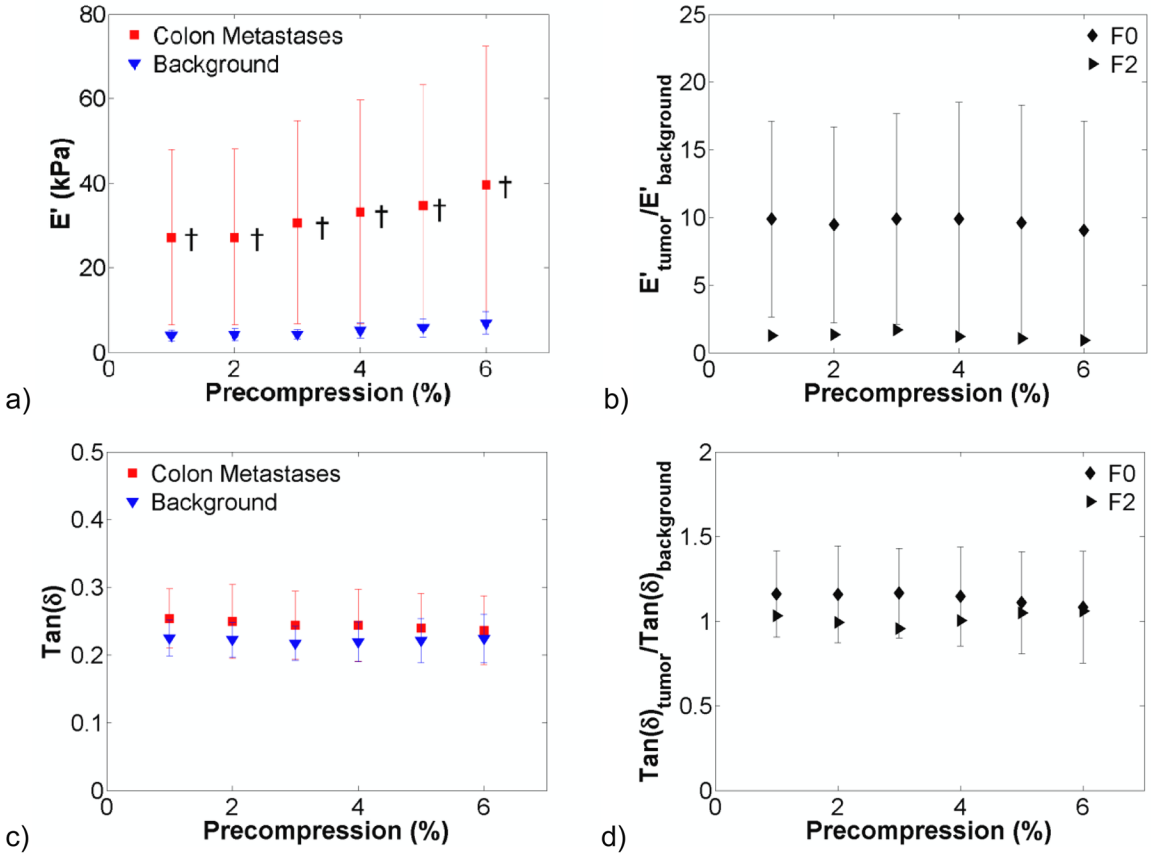

Figure 4.

Viscoelastic properties of colon metastases (n = 6). The storage modulus (a) of the malignant tissue was much higher in colon metastases and exhibited higher variability than the surrounding background tissue (†, $p<0.05$; ‡, $p<0.001$). Storage modulus contrast (b) was relatively constant, as were tan(δ) (c) and tan(δ) contrast (d).

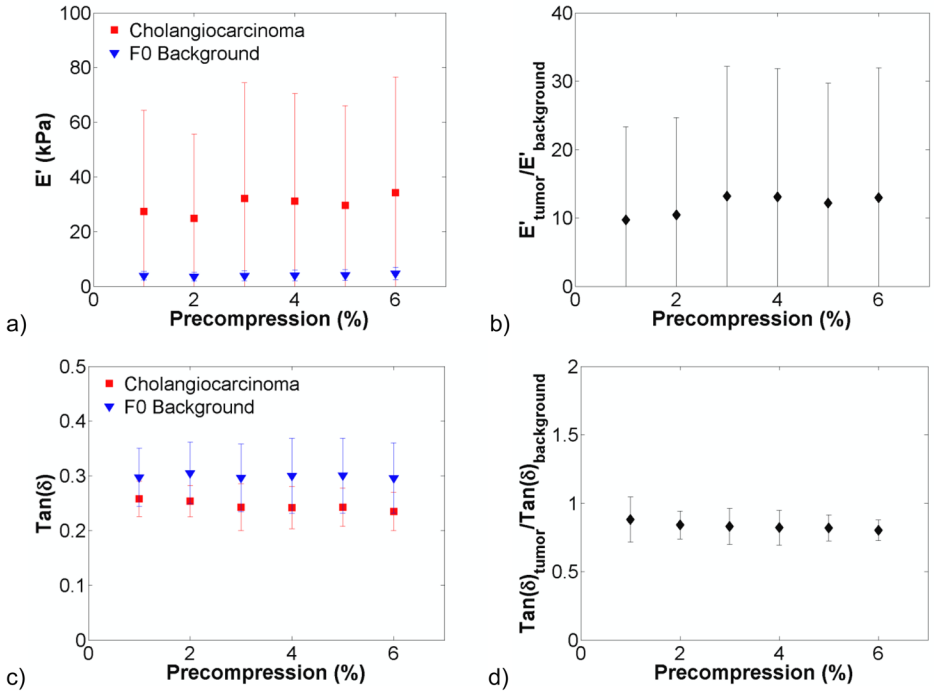

Figure 5.

Viscoelastic properties of cholangiocarcinomas (n = 3). The storage modulus (a) was higher and more variable in the malignant tissue than the F0 background. Storage modulus contrast (b) was relatively constant, as were tan(δ) (c) and tan(δ) contrast (d).

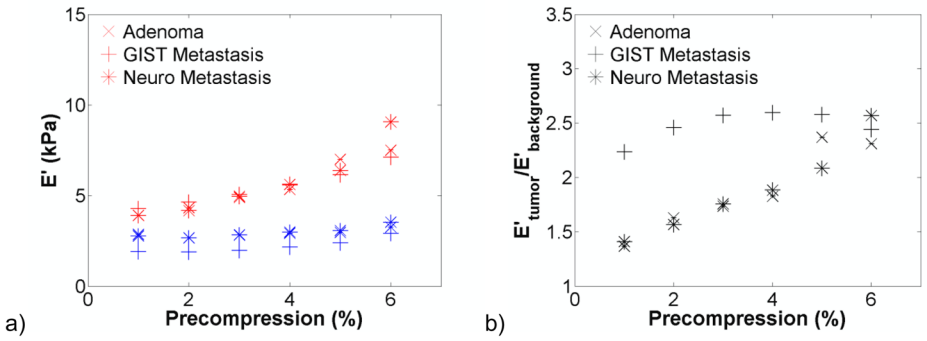

Figure 6.

Effects of precompression on a benign adenoma (n = 1), gastrointestinal stromal (GIST) metastasis (n = 1), and neuroendocrine (Neuro) metastasis (n = 1). The lesion and normal tissue storage modulus (a) increased with increasing precompression. An increase in contrast (b) with increasing precompression was observed in the adenoma and the neuroendocrine metastasis.

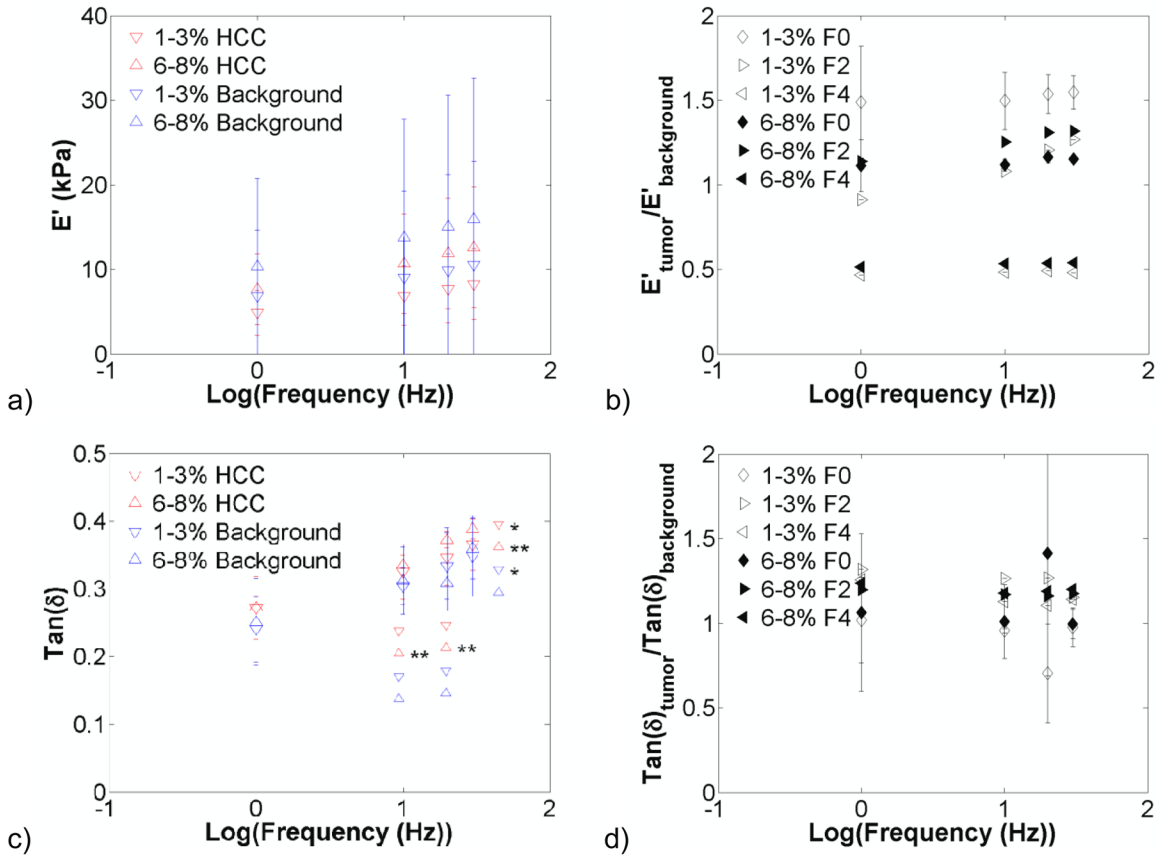

Figure 7.

Effects of testing frequency on hepatocellular carcinoma (HCC) and surrounding background viscoelastic properties (n = 4). Graphs present the storage modulus (a), modulus contrast (b), tan(δ) (c), and tan(δ) contrast (d) for the 1–3% and 6–8% compression ranges. Increases in frequency increased the storage modulus and tan(δ) (*, $p<0.05$; **, $p<0.001$). Storage modulus and tan (δ) contrast remained relatively constant with increases in frequency. Note: symbols to the left of the asterisks indicate statistical significance only – i.e. they are not actual data points.

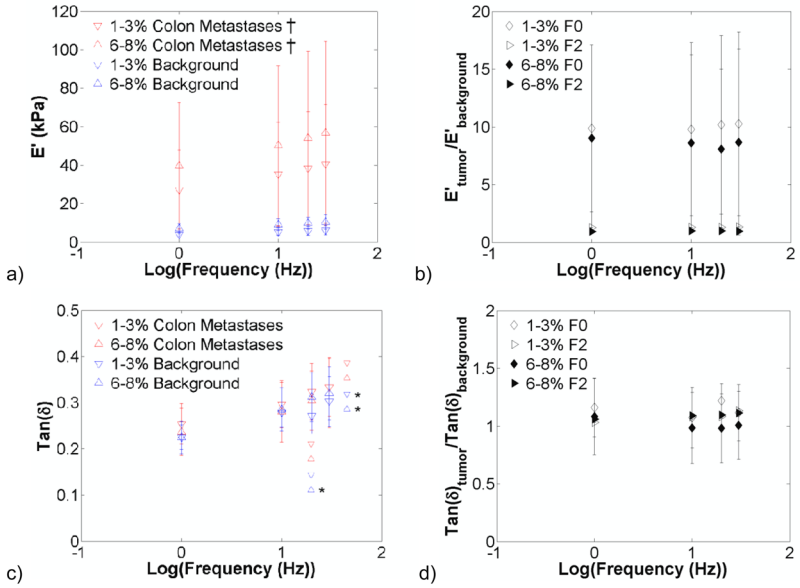

Figure 8.

Effects of frequency on colon metastases and surrounding background viscoelastic properties (n = 6). Graphs present the storage modulus (a), modulus contrast (b), tan(δ) (c), and tan(δ) contrast (d) for the 1–3% and 6–8% compression ranges. The storage modulus of colon metastases was significantly higher than the background for all precompression levels at all frequencies (†, $p<0.05$; ‡, $p<0.001$). Increases in frequency increased the storage modulus and tan(δ) (*, $p<0.05$; **, $p<0.001$). Storage modulus and tan (δ) contrast in colon metastases remained relatively constant with increases in frequency. Note: symbols to the left of the asterisks indicate statistical significance only – i.e. they are not actual data points.

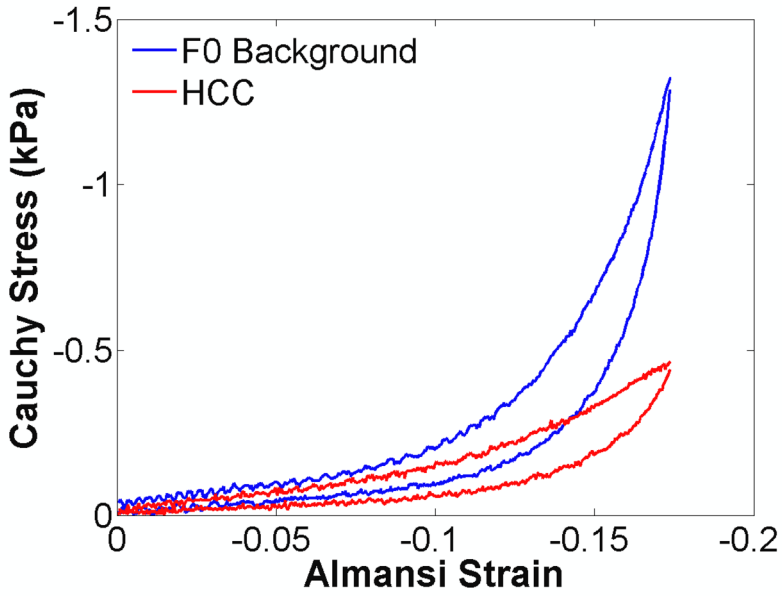

Figure 9.
Third ramp testing cycle of a hepatocellular carcinoma and surrounding F0 background tissue compressed up to 20%. Interestingly, the background tissue strain-hardened faster than the primary tumour.

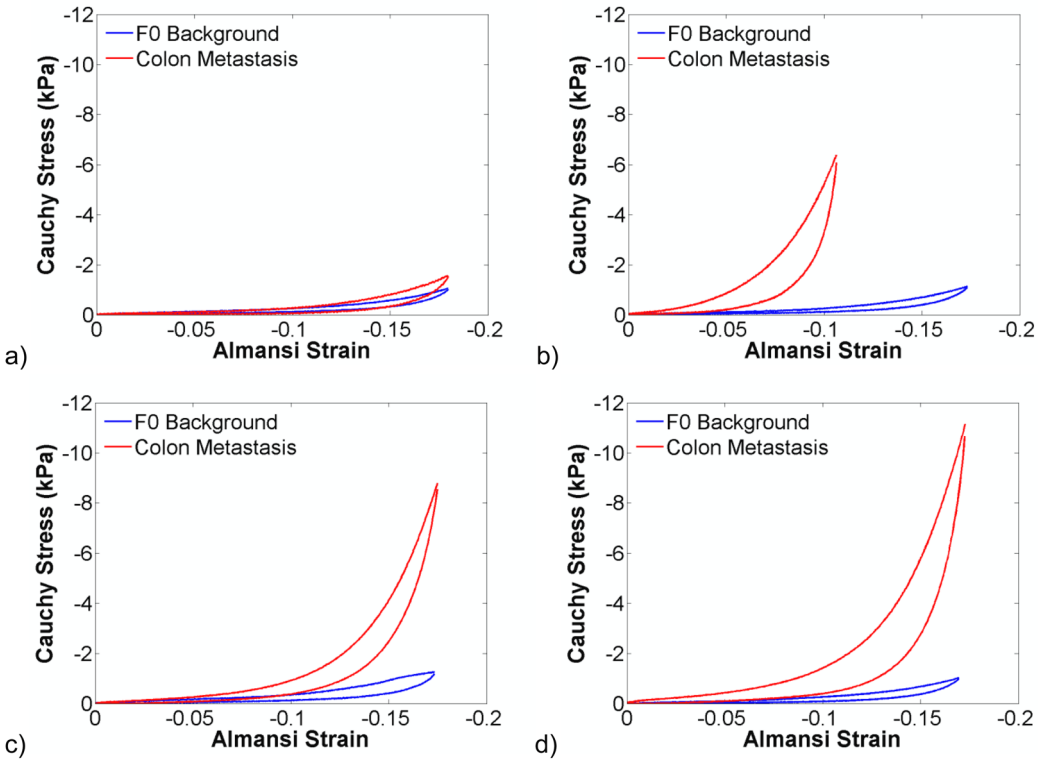

Figure 10.
Third ramp testing cycle of colon metastases and surrounding F0 background tissue compressed up to 20% (n = 4). There was significant variability in the strain hardening of the colon metastases that were tested (a–d). However, in all cases, the secondary tumour hardened faster than the background tissue.

Table 1

Liver Pathologies Mechanically Tested

Pathology			**Fibrosis Score**				**Fatty Liver**
Lesion	**N**	**F0**	**F1**	**F2**	**F3**	**F4**	**Steatosis**
Colon Metastases	6	5	0	1	0	0	2
Hepatocellular Carcinoma	4	2	0	1	0	1	1
Cholangiocarcinoma	3	3	0	0	0	0	1
Gastrointestinal Stromal Metastases	1	1	0	0	0	0	0
Neuroendocrine Metastases	1	1	0	0	0	0	1
Adenoma	1	1	0	0	0	0	0
Total:	16	13	0	2	0	1	5
Additional Backgrounds:	--	1	0	0	0	1	1
Cumulative Total:	16	14	0	2	0	2	6